DOI:10.21276/sjeat

Saudi Journal of Engineering and Technology
Scholars Middle East Publishers
Dubai, United Arab Emirates
Website: http://scholarsmepub.com/

ISSN 2415-6272 (Print)
ISSN 2415-6264 (Online)

Original Research Article

Effect of Temperature on The Bioleaching of Iron from Silica Sand with *Aspergillus niger* Correlated with Shrinking Core and Mixed Kinetic Models

O. C. N. Ndukwe*, T. F. Eze
Department of Chemical Engineering, Federal University of Technology Owerri, P. M. B 1526, Imo State, Nigeria

***Corresponding Author:**
O. C. N. Ndukwe
Email: ndukwe486@gmail.com

Abstract: The influence of temperature on the bioleaching of iron from silica sand with *Aspergillus niger* has been studied with three size fractions of silica sand: +120-212µm, +212-300µm, and +300-425µm over the temperature range 40 to 80^0C for several hours. The experimental data were fitted to the shrinking core model (ash layer diffusion control and chemical reaction control) and a mixed kinetic model that incorporates a multiplying factor, b. Optimal temperature for bioleaching was found to be 70^0C and the amount of iron leached increased with decreasing particle size, with +120-212µm being the most effective particle size fraction. The shrinking core model with chemical reaction control and ash layer diffusion control failed to explain the effect of temperature on the kinetics of bioleaching. The mixed kinetic model with the multiplying factor b=0.2 gave a perfect fit to the experimental data after the second hour of bioleaching. At the early part of the bioleaching process where the mixed kinetic model failed, ash layer diffusion seemed to be in control. Based on our work, a staged bioreactor design that relies on the ash layer and mixed kinetics models may be required for the process.

Keywords: Silica sand, *Aspergillus niger*, Bioleaching, Iron, Shrinking core, Mixed Kinetics, Model, Temperature.

INTRODUCTION

Silica sand which is the main component of all types of standard and specialty glass provides the essential Silicon Oxide (SiO_2) whose chemical purity is the primary determinant of colour, clarity and strength of glass [1]. Naturally occurring silica sand contains various iron and clay materials which coat silicate grains or are impregnated in silica matrix, but the iron in the silica sand must be removed or reduced to an acceptable level for it to be used for glass production. Processes for reducing iron such as beneficiation, heat treatment, acid wash, gravity settling and floatation are energy intensive, not eco-friendly, expensive, and even the chemicals used are hazardous. This has encouraged alternative means of purifying silica sand.

Several researchers have demonstrated that various microorganisms participate in metal extraction, metal concentration, metal detoxification and desulphurization processes [2-6]. Studies have shown *Aspergillus niger* to be very effective in removal of iron from silica sand [4, 7-9]. The interest in bioleaching process has increased because it is expected to be a viable option in place of the conventional heat/chemical treatment methods as the kinetics becomes well understood. Mustafa *et al* [10] have shown that contact time, pH, incubation temperature and carbon source play important role in the bioleaching of iron from silica sand; this agrees with an earlier study by Ndukwe and Chikwendu [9].

The shrinking core model has been used to describe the process of bioleaching at room temperature by some researchers [11-15].This model of bioleaching proposes that at any point in time, there is an unreacted core of the metal being leached which shrinks during reaction with the non-complexing or weak complexing acid produced by the organism. The shrinking core equations (1), (2) and (3) represent the film diffusion, chemical reaction and ash layer diffusion controls respectively.

$$K_f t = X \qquad (1)$$

$$K_r t = 1 - (1 - X)^{1/3} \qquad (2)$$

$$K_d t = 1 - \frac{2}{3}X - (1 - X)^{2/3} \qquad (3)$$

Where X is the conversion fraction of solid particles, in this case iron, K_f, K_r and K_d are the apparent rate constants for film diffusion, surface

chemical reaction and ash layer diffusion controls respectively, and t is the reaction time.

Ndukwe and Uchendu [14] applied the shrinking core model (chemical reaction and ash layer controls) to the kinetics of bioleaching of iron from silica sand by *Aspergillus niger* at room temperature of about 30^0C. Lizama *et al* [12] had applied the model to bioleaching of metals by bacteria. In all, the shrinking core failed to describe the kinetics of bioleaching fully. In this work that dwells on the influence of temperature, we have used the chemical reaction and ash layer controls equations, as well as equation (4), the mixed kinetic model [16], which is a combination of the conversion terms of the chemical reaction and ash layer diffusion equations.

$$K_m t = 1 - \frac{2}{3}X - (1-X)^{2/3} + b\left(1 - (1-X)^{1/3}\right) \quad (4)$$

Where K_m is the apparent rate constant, b is the multiplying factor, while X and t retain their definitions given earlier. The change in proportion of the dominating reaction mechanism was established by setting the values of "b" in equation (4) between 0 and 1. Small value of b means that ash layer diffusion is a more dominant process, while high value of b indicates that chemical reaction dominates. The choice of "b" was based on the value that gave the highest coefficient of determination (R^2) when the experimental data were fitted to the mixed kinetic model.

EXPERIMENTAL SECTION

Initial Concentration of Iron in the Silica Sand

About 5kg of naturally occurring silica sand was obtained from Otammiri River in Owerri West Local Government Area, Imo State, Nigeria. The sample was washed with deionized water to remove clay particles and other unwanted materials adhering to the surface of the sand, after which it was dried for 3-days and separated into different particle size fractions with the aid of a set of manual sieves. Three different particle size fractions +120 - 212µm, +212µm - 300µm and +300 - 425µm were selected for the experiments. The presence of iron was determined by the Thiocyanide solution method. Standard solutions containing 0.5 to 2.5mg/ml of Iron (III) were prepared and the absorbance of the solutions was determined with the aid of a UV/Visible spectrophotometer (Searchtech 755S (UK)). The relationship between concentration of iron in the standard solution and absorbance was established with the measured data, and used subsequently to determine the concentration of iron in the Silica sand and in the leachate. 2g of silica sand from the first particle size range (+120 -212µm) was weighed and transferred into a 250ml conical flask containing 25ml of 8M HNO_3 (KERMEC) and made up to 100ml with distilled water. The mixture was agitated for about 5 minutes and subjected to digestion for about 60 minutes. The solution was cooled and then filtered into 100ml standard flask, after which 10ml of it was pipetted and its absorbance determined using the UV/Visible spectrophotometer (Searchtech 755S(UK)) at a wavelength of 510nm. This experiment was repeated for the particle size fraction +212µm - 300µm, and +300 - 425µm. The results are given in table 1.

Fungi Isolation, cultivation and Identification

The fungus was isolated from the soil at a refuse dump in Owerri, Imo State, Nigeria. The culture Sabouraud Dextrose Agar (SDA) (TM, MEDIA, India) medium was prepared according to the manufacturer's instruction. 62g of the SDA was dissolved in 1000ml of distilled water and stirred thoroughly to ensure proper homogenization. It was allowed to soak for 10 minutes, mixed and sterilized by autoclaving at 121^oC for 15minutes and was cooled to 45^0C before pouring into sterile petri-dishes. 1g of the soil sample was weighed and dissolved in 9ml of sterilized formal saline. 0.1ml was pipetted out and spread evenly on solidified SDA, and incubated at 30^0C for about 7 days, so that adequate number of spores formed. The fungal isolate was identified based on its morphology and colour of the surface of the colony using fungal identification guidelines described by Samson *et al* [17]. For microscopic identification, wet mounts of the isolate were prepared using lacto phenol cotton blue. A drop of the lacto phenol cotton blue was placed on a sterile grease-free slide with a sterile dissecting needle. A small portion of the inoculum was collected and tested on the slide. The sample was covered with a cover slip and examined under microscope to observe hypha cells and spores. The spore suspension was diluted with deionized water and standardized to 2 x 10^8 spores/ml of suspension.

Bioleaching

2.0g of silica sand from the particle size fraction, +120 - 212µm, was weighed into 250ml conical flask containing 150ml of prepared medium which contained Sucrose (KERMEC) 100g/l; NH_4NO_3 (AVIS Chemicals 99%) 450mg/l; KH_2PO_4 (KERMEC) 100mg/l; $MgSO_4.7H_2O$ (KERMEC) 300mg/l; $FeSO_4.7H_2O$ (GFS Chemical) 0.1mg/l; $ZnSO_4$ (KERMEC) 0.25mg/l as culture medium. The flask was plugged with a non-absorbent cotton and then sterilized in an autoclave (Searchtech YA-208A) for 20 minutes at 121^0C. It was then inoculated with 2ml of *Aspergillus niger* spore suspension (2 x 10^8 spores/ml) and agitated for 20 minutes to achieve a good degree of homogeneity between the fungi and the sand. The flask was incubated in an oven (DHG 9101-USA) at a temperature of 40^0C and monitored for 7 hours. At a

regular interval of 1 hour, 10ml of the leachate from the flask was obtained, filtered, and digested to stop further microbial actions. The concentration of iron leached out was then determined with the UV/Visible spectrophotometer, after which the fractional conversion of the iron was calculated. The experiment was repeated at the temperatures of 50^0C, 60^0C, 70^0C, and 80^0C. A similar experiment was done with +212µm - 300µm, and +300 - 425µm sand size fractions. The results are given in tables 2, 3 and 4. The fractional conversions have been plotted against time for each of the particle size fractions at varying temperatures as shown in figs. 1, 2 and 3. Fig. 4 gives the overall fraction of iron leached out for the three size fractions, +120 - 212µm, +212µm - 300µm, and +300 - 425µm at different temperatures.

Kinetics of Bioleaching

The fractional conversions of the experimental data in tables 2, 3 and 4 were fitted to equations (2), (3) and (4) to obtain the reaction rate constants K_r, K_d and K_m for chemical reactions control, ash layer diffusion control and mixed kinetics control respectively. The choice of 'b', the multiplying factor (b=0.2), for the mixed kinetic model was based on the value that gave the highest coefficient of determination (R^2 = 0.984) when the experimental data with varying values of b were fitted to equation (4). The reaction rate constants were then employed numerically with the equations to predict the fractional conversion of iron at 70^0C, since from experiment (fig 4), it was the optimal temperature for bioleaching. A MATLAB program was written for the purpose. The results are given in table 5 and fig. 5.

RESULTS AND DISCUSSION

Effects of Temperature

Table 1 shows that it was possible to locate the highest amount of iron (45.045g/g sand) in the sand matrix with the smallest sand fraction (+120-212µm); the amount of iron identifiable decreased with increase in the size fraction. Since initial concentration of iron fell with increased sand size fraction, being 43.568mg/g sand for +212-300µm and 39.189mg/g sand for +300-425µm, the effectiveness of *Aspergillus niger* in the removal of iron from silica sand will be enhanced by beneficiating the sand. Figs 1, 2 and 3 show that temperature, to a good extent, positively influences the bioleaching of iron from silica sand by *Aspergillus niger*. The rate of bioleaching of iron is approximately the same with all the size fractions. The highest leaching rate occurred in the first hour of bioleaching for all size fractions and temperatures. Figs 1,2,3 and 4 show that 70^0C is the optimal temperature for bioleaching of iron from silica sand with *Aspergillus niger*, since at this temperature, the maximum conversion fraction was achieved irrespective of the sand size fraction. When the temperature was increased to 80^0C, the amount of iron leached fell, not minding the sand size fraction. The kinetics of the bioleaching process was then verified with the sand size fraction +120-212µm at 70^0C. With the sand size fraction +120-212µm at 70^0C, the reaction rate constants obtained by fitting experimental data to the shrinking core model (chemical reaction and ash layer diffusion controls) and the mixed kinetic model, as well as their coefficients of determination, R^2, were as follows: K_r = 0.01326 (R^2 = 0.931), K_d = 0.00142 (R^2 = 0.963) and K_m = 0.00407 (R^2 = 0.984).

Fig. 5 and table 5 with which we can compare experimental data with predicted, based on ash layer diffusion control, chemical reaction control and the mixed kinetic model, were obtained by using the appropriate reaction rate constants to solve numerically for conversion fractions in equations (2), (3) and (4). Fig 5 shows that the mixed kinetic model gives a perfect prediction of experimental data between the third hour and seventh hour. Ash layer diffusion prediction agrees with the experimental data within the first two hours but subsequently fails to give a good prediction. Chemical reaction control fails completely. The mixed kinetic model is much better than the shrinking core model in trying to account for the effect of temperature on bioleaching of iron from silica sand. However, the mixed kinetic model does not adequately predict the initial process of bioleaching where it is considered that cell solubilisation may take place. A bioreactor design that is based wholly on the mixed kinetic model for purification of iron from silica sand may not yield the desired result. However, for the particle size we worked on, and at 70^0C, a combination of the ash layer control and the mixed kinetic model may be adequate.

Table 1: Initial Concentrations of Iron in 2g Silica Sand of various Particle Sizes

PARTICLE SIZE (µm)	INITIAL CONC. OF IRON(mg/g sand)
+120-212µm	45.045
+212-300µm	42.568
+300-425µm	39.189

Table 2: Concentration of iron in silica sand leachate and its fractional conversion with time and temperature for particle size +120-212µm

	40^0C			50^0C			60^0C			70^0C			80^0C		
TIME (HRS)	**Leachate Absorb. From (UV)**	**Iron in Leachate (mg/ml)**	**Conv. fraction (X)**	**Leachate Absorb. From (UV)**	**Iron in Leachate (mg/ml)**	**Conv. fraction (X)**	**Leachate Absorb. From (UV)**	**Iron in Leachate (mg/ml)**	**Conv. fraction (X)**	**Leachate Absorb. From (UV)**	**Iron in Leachate (mg/ml)**	**Conv. fraction (X)**	**Leachate Absorb. From (UV)**	**Iron in Leachate (mg/ml)**	**Conv. fraction (X)**
0	0.000	0.000	0.0000	0.000	0.000	0.0000	0.0000	0.000	0.0000	0.0000	0.000	0.0000	0.0000	0.000	0.0000
1	0.012	2.478	0.0550	0.016	3.378	0.0750	0.020	4.279	0.0950	0.025	5.405	0.1200	0.024	5.180	0.1150
2	0.016	3.378	0.0750	0.020	4.279	0.0950	0.025	5.405	0.1200	0.031	6.757	0.1500	0.028	6.081	0.1350
3	0.021	4.505	0.1000	0.025	5.405	0.1200	0.030	6.532	0.1450	0.034	7.432	0.1650	0.032	6.982	0.1550
4	0.027	5.856	0.1300	0.033	7.207	0.1600	0.036	7.883	0.1750	0.041	9.009	0.2000	0.037	8.108	0.1800
5	0.036	7.883	0.1750	0.040	8.784	0.1950	0.043	9.459	0.2100	0.046	10.135	0.2250	0.044	9.685	0.2150
6	0.041	9.009	0.2000	0.045	9.910	0.2200	0.051	11.261	0.2500	0.053	11.712	0.2600	0.052	11.486	0.2550
7	0.047	10.360	0.2300	0.051	11.261	0.2500	0.055	12.162	0.2700	0.059	13.063	0.2900	0.057	12.613	0.2800

Table 3: Concentration of iron in silica sand leachate and its fractional conversion with time and temperature for particle size +212-300µm

	40^0C			50^0C			60^0C			70^0C			80^0C		
TIME (HRS)	**Leachate Absorb. From (UV)**	**Iron in Leachate (mg/ml)**	**Conv. fraction (X)**	**Leachate Absorb. From (UV)**	**Iron in Leachate (mg/ml)**	**Conv. fraction (X)**	**Leachate Absorb. From (UV)**	**Iron in Leachate (mg/ml)**	**Conv. fraction (X)**	**Leachate Absorb. From (UV)**	**Iron in Leachate (mg/ml)**	**Conv. fraction (X)**	**Leachate Absorb. From (UV)**	**Iron in Leachate (mg/ml)**	**Conv. fraction (X)**
0	0.000	0.000	0.0000	0.0000	0.000	0.0000	0.0000	0.000	0.0000	0.0000	0.000	0.0000	0.0000	0.000	0.0000
1	0.010	2.027	0.0476	0.014	2.928	0.0688	0.015	3.153	0.0741	0.018	3.829	0.0900	0.016	3.378	0.0794
2	0.013	2.702	0.0635	0.016	3.378	0.0794	0.019	4.054	0.0953	0.023	4.955	0.1164	0.021	4.505	0.1058
3	0.017	3.604	0.0847	0.020	4.279	0.1005	0.023	4.955	0.1164	0.027	5.856	0.1376	0.025	5.405	0.1270
4	0.021	4.505	0.1058	0.025	5.405	0.1270	0.028	6.081	0.1429	0.032	6.982	0.1640	0.030	6.532	0.1534
5	0.026	5.631	0.1323	0.030	6.532	0.1534	0.033	7.207	0.1693	0.037	8.108	0.1905	0.035	7.658	0.1799
6	0.031	6.757	0.1587	0.035	7.658	0.1799	0.039	8.559	0.2011	0.042	9.234	0.2169	0.040	8.784	0.2063
7	0.035	7.658	0.1799	0.039	8.559	0.2011	0.043	9.459	0.2222	0.048	10.586	0.2487	0.045	9.910	0.2328

Table 4: Concentration of iron in silica sand leachate and its fractional conversion with time and temperature for particle size +300-425µm

	40^0C			50^0C			60^0C			70^0C			80^0C		
TIME (HRS)	**Leachate Absorb. From (UV)**	**Iron in Leachate (mg/ml)**	**Conv. fraction (X)**	**Leachate Absorb. From (UV)**	**Iron in Leachate (mg/ml)**	**Conv. fraction (X)**	**Leachate Absorb. From (UV)**	**Iron in Leachate (mg/ml)**	**Conv. fraction (X)**	**Leachate Absorb. From (UV)**	**Iron in Leachate (mg/ml)**	**Conv. fraction (X)**	**Leachate Absorb. From (UV)**	**Iron in Leachate (mg/ml)**	**Conv. fraction (X)**
0	0.000	0.000	0.0000	0.0000	0.000	0.0000	0.0000	0.000	0.0000	0.0000	0.000	0.0000	0.0000	0.000	0.0000
1	0.008	1.577	0.0402	0.011	2.252	0.0575	0.014	2.928	0.0747	0.016	3.378	0.0862	0.015	3.009	0.0768
2	0.010	1.852	0.0473	0.014	2.928	0.0747	0.017	3.604	0.0920	0.021	4.505	0.1149	0.019	3.935	0.1004
3	0.013	2.546	0.0650	0.017	3.604	0.0920	0.020	4.279	0.1092	0.025	5.405	0.1379	0.023	4.861	0.1240
4	0.019	3.935	0.1004	0.022	4.730	0.1207	0.025	5.405	0.1379	0.029	6.306	0.1609	0.027	5.787	0.1477
5	0.024	5.093	0.1300	0.027	5.856	0.1494	0.031	6.750	0.1724	0.034	7.432	0.1897	0.033	7.176	0.1831
6	0.028	6.019	0.1536	0.030	6.532	0.1667	0.035	7.658	0.1954	0.039	8.559	0.2184	0.037	8.102	0.2067
7	0.031	6.713	0.1713	0.033	7.207	0.1839	0.038	8.333	0.2126	0.043	9.459	0.2414	0.041	9.028	0.2304

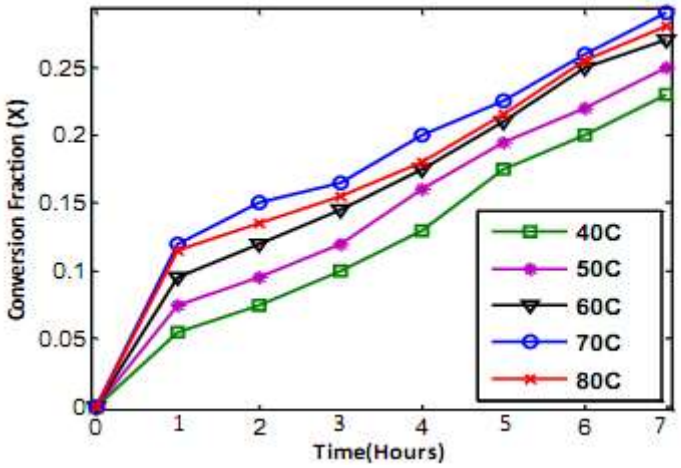

Fig-1: Fraction of Iron leached with Time at different Temperatures for Size fraction +120 - 212µm

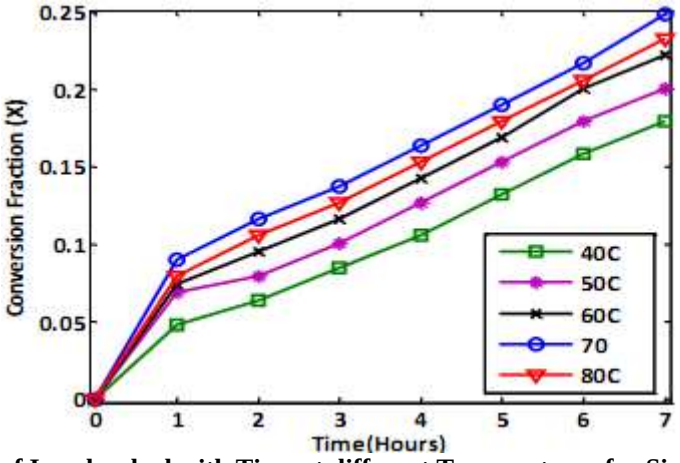

Fig-2: Fraction of Iron leached with Time at different Temperatures for Size fraction +212 - 300µm

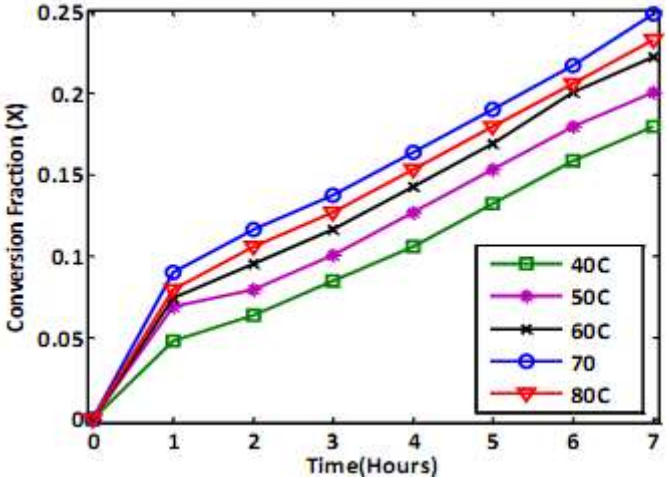

Fig-3: Fraction of Iron leached with Time at different Temperatures for Size fraction +300 - 425µm

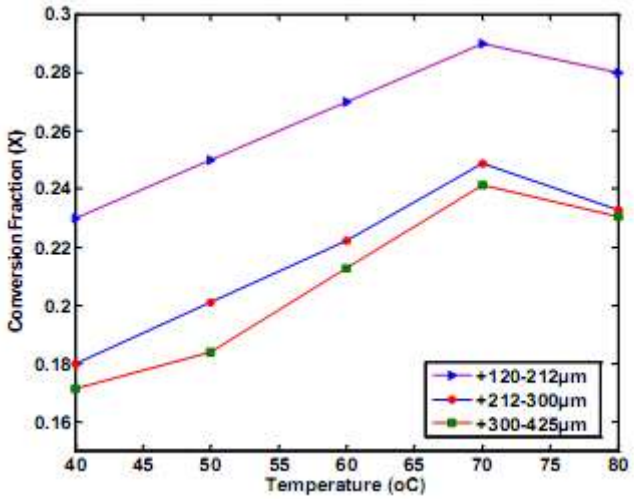

Fig-4: Overall Fraction of Iron leached out after 7 hours at different Temperatures with different Size fractions

Table 5: Fractional Conversions predicted by the Ash Layer Diffusion Control, Chemical Reaction Control and the Mixed Kinetic Model at 70^0C with +120-212µm

Time (Hrs)	Conv. fract. ($X_{expt.}$)	Conv. fract. ($X_{pred.}$) Ash Layer	Conv. Fract. ($X_{pred.}$) Chem. Rxn	Conv. Fract. ($X_{pred.}$) Mixed Model
0	**0.0000**	0.0000	0.0000	0.0000
1	**0.1200**	0.1091	0.0494	0.0629
2	**0.1500**	0.1526	0.0972	0.1145
3	**0.1587**	0.1854	0.1433	0.1587
4	**0.2000**	0.2126	0.1878	0.1978
5	**0.2337**	0.2362	0.2308	0.2331
6	**0.2652**	0.2572	0.2722	0.2652
7	**0.2948**	0.2764	0.3121	0.2948

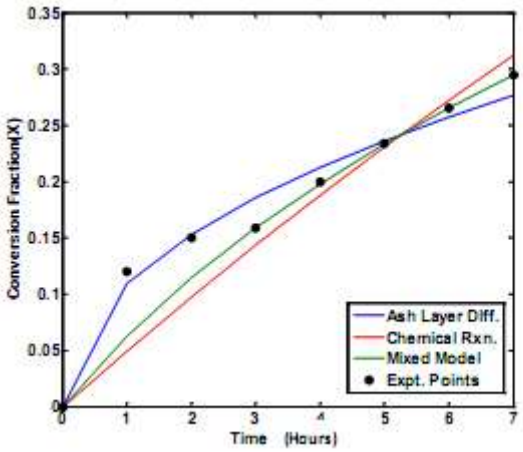

Fig-5: Comparison of the Experimental Conversion Fraction (Xexpt) with the predicted Conversion Fraction (Xpred.) for Size fraction +120-212µm at 700C

CONCLUSION

An optimal temperature of 70^0C has been found for the bioleaching of iron from silica sand by *Aspergillus niger;* above and below this temperature, the fraction of iron leached fell. The shrinking core model (chemical reaction control and ash layer diffusion control) could not describe fully the influence of temperature on bioleaching. The mixed kinetic model with multiplying factor b = 0.2 gave a perfect fit to the experimental data after the first two hours of the bioleaching process. Neither the shrinking core nor the mixed kinetic model alone could describe the kinetics.

A staged bioreactor design, based on the mixed kinetic model and the ash layer diffusion control is required for this bioleaching process.

REFERENCES

1. Nigerian Industrial Sand Association. (2011). *Industrial Sand*. NISA, 1.
2. Styriakiova, L., Styriak, I., Malchoosky, P., Vecera, Z., & Kolousek, D. (2007). Bacterial Clay Release and Iron Dissolution during the Quality Improvement of Quartz Sand, *Hydrometallurgy*, *89*(1&2), 99-106.
3. Wahab, G. M. A., Amin, M. M., & Aita, S. K. (2012). Bioleaching of Uranium-bearing Material from Abu Thor area, West Central Sinai, Egypt for Recovering Uranium. *Arab Journ. of Nuclear Sciences and Applications*, *45*(2), 169-178.
4. Bayat, O., Arslan, V., & Bayat, B. (2011). Use of *Aspergillus niger* in the Bioleaching of Colemanite for the Production of Boric acid. *Electronic Journal of Biotechnology*, *14*(3).
5. Xu, T., Ramanathan, T., & Ting, Y. (2014). Bioleaching of Incinerated fly ash by Aspergillus Niger-precipitation of Metallic Salt Crystals and Morphological Alteration of the Fungus. *Biotech Reports*, *3*, 8-14.
6. Raistrick, H., & Clark, A. B. (1919). On the Mechanism of Oxalic Acid Formation by *Aspergillus niger*. *Biochem J.*, *13*(4), 329-344.
7. Mandal, S. K., & Barnejee, P. C. (2003). Leaching of Iron from China Clay with Oxalic Acid: Effect of Acid concentration, pH, Temperature, Solids Concentration and Shaking. Proceedings of the 15th International Biohydrometalurgy Symposium, Athens, Hellas, Sept.14th-15th, 291-302.
8. Xu, T., & Ting, Y. (2003). Optimization Study on Bioleaching of Municipal Solid Waste (MSW) Incineration Fly Ash by A. *Niger*, Proceedings of the 15th International Biohydrometalurgy Symposium, Athens, Hellas, Sept.14th -15th , 329-336.
9. Ndukwe, O. C., & Chikwendu, C. (2010). Bioleaching of Silica Sand with the Fungi Fosarium Oxysporum, Peninicillium *notatum*, *Aspergillus niger* and *Rhizopus*, *Advances in Science and Technology*, *4*(2), 125-130.
10. Mustafa, M. K. A., Bader, D. N., Khachiek, T. V., Fleah, I. K., & Issa, I. G. (2011). Biobeneficiation of Silica Sand for Crystal Glass Industry from Ardhuma Location, Iraqi Western Desert. *Iraqi Bulletin of Geology and Mining*, *7*(1), 77-86.
11. Szubert, A., Lupinski, M., & Sadowski, Z. (2006). Application of Shrinking Core Model to Bioleaching of Black Shale Particles. *Physicochem Probl of Miner of Miner. Process*, *40*, 211-225.
12. Lizama, H. M., Fairweather, M. J., Dai, Z., & Allegretto, T. D. (2003). How does bioleaching start? *Hydrometal.*, *69*(1-3), 109-116.
13. Safari, V., Arzpeyma, G., Kashchi, F., & Mostoufi, N. (2009). A Shrinking Particle-Shriniking Core Model for Leaching of a Zinc Ore Containing Silica. *Int. J. of Miner. Process*, *93*(1), 79-83.
14. Ndukwe, O. C., & Uchendu, C. E. (2012). Shrinking Core Model applied to the Bioleaching of Iron from Silica sand. *Intl. Journal of Academc Research*, *4*(4), 183-188.
15. Sadowski, Z., & Szubert, A. (2010). Modelling of Bioleaching Kinetics of Black Shale Ore Based on Changes of the Surface Area. *Chem. And Process Eng.*, *31*, 107-118.
16. Sultana, U. K., Gulshan, F., & Kury, A. S. (2014). Kinetics of Leaching of Iron Oxide in Clay in Oxalic Acid and in Hydrochloric Acid Solutions. *Material science and Metalurgical Eng.*, *2*(1), 5-10.
17. Samson, R. A., Houbraken, J., Summerbell, R. C., Flannigan, B., & Miller, J. D. (2001) Common and important species of fungi and actinomycetes in indoor environments, *Microogranisms in Home and Indoor Work Environments*. CRC, 287–292.
18. Feng, Q., Wen, C., Wang, Y., Zhao, W., & Deng, J. (2015). Investigation of Leaching Kinetics of Cerussite in Sodium Hydroxide Solutions. *Physicochem. Probl. Miner. Process*, *51*(2), 491-500.
19. Mustafa, M. K. A. (2008). Biobenefication of Silica Sand for Optical Glass Production Using *Aspergillus niger*. *GEOSURV. Int. rep.* no. 3107
20. Basset, J., Denny, R. C., Jeffery, G. H., & Mendham, J. (1986). Vogel's Textbook of Quantitative Inorganic Analysis. London. Longman Ground Ltd, 23-125.
21. British Standards Methods: Sampling and analysis of glass making sands. (2008). *BSI*, 1-30